Egyptian Journal of Archaeological and Restoration Studies
An international peer-reviewed journal published bi-annually
www.ejars.sohag-univ.edu.eg

Original Article

A PRELIMINARY EXPERIMENTAL STUDY FOR THE TREATMENT OF A REPLICA OF TUTANKHAMUN'S BOUQUET

Khalifa N.[1(*)], El Hadidi N.[2], Hamdy R.[3], Abd El-sadek M.S.[4] & Mohamed, W.[5]

[1]*Royal Carriage Museum, Ministry of Tourism & Antiquities, Egypt*
[2]*Organics Conservation dept., Faculty of Archaeology, Cairo Univ., Giza, Egypt*
[3]*Botany & Microbiology dept., Faculty of Science, Cairo Univ., Giza; Biological Sciences dept., Faculty of Science, Galala Univ., Galala University, New Galala City, Suez*
[4]*Nanomaterial Lab., Physics dept., Faculty of Science, South Valley Univ., Qena, Egypt; Physics dept. Faculty of Science, Galala Univ., New Galala City, Suez*
[5] *Ministry of Tourism & Antiquities, Egypt*
E-mail address: nogagomammm21@gmail.com

Article info.

Article history:
Received: 21-1-2025
Accepted: 15-7-2025
Doi: 10.21608/ejars.2026.499294

Keywords:
Persea
Olive
Klucel E
Plant extracts
Green conservation
MgO NPs
ZnO NPs

EJARS – Vol. SI (1) – April 2026: SI 63-SI 74

Abstract:
Plant fibers are organic materials that require advanced conservation strategies to ensure their long-term preservation and stability. Although plant-based materials are widely used in archaeological artifacts, there are very few studies that focus specifically on how to treat and preserve them. Therefore, this study aims to evaluate the use of green, nanoparticle-based treatments on three common types of leaves found in ancient floral bouquets—namely persea, olive, and date palm—by using visual inspection, pH, color change and contact angle measurements, in addition to ATR-FTIR analysis. This preliminary study highlights the potential of Klucel E combined with plant extracts and nanoparticles (NPs) as an effective conservation strategy for plant leaves. Visual assessment and examination of the samples revealed distinct color changes and variations unique to each plant type. The absorption of the treated fibers to the consolidation materials, is confirmed in the ATR-FTIR spectra by the increase in intensity due to the application of treatment materials. The results demonstrated significant changes in the surface morphology, and moisture resistance of the treated fibers, with variations depending on the leaf type. Olive leaves exhibited the most pronounced color changes, particularly with the addition of MgO NPs and ZnO NPs, while minimal color changes were observed in persea leaves. However, pH measurements confirmed that the applied treatments contributed to a chemically stable environment, supporting the preservation process. Among all tested formulations, the most effective treatment was Klucel E combined with plant extract, followed by Klucel E with plant extract and MgO NPs.

1. Introduction

Ancient Egyptian civilization is renowned for its artistry in floral design and the diverse uses of flowers reflected in the artifacts found in ancient tombs. Various paintings and sculptures depict the significance of flowers in their society, and historical texts reveal how the ancient Egyptians utilized and interacted with flowers and ornamental plants. They selected flowers and plants that thrived in the Nile Valley, such as the sacred lotus, palms, and papyrus, among others. The ancient Egyptians were particularly fond of colors, incorporating lively hues of red, yellow, green, and blue in their floral designs. Flowers were not only used for personal adornments such as in necklaces and wreaths—but also served as decorative elements in vases and bowls and offerings during religious festivals and other significant occasions, often presented as beautiful bouquets [1]. The art of making bouquets has evolved through several distinct phases over time. In its initial form, during the Predynastic period, bouquets typically consisted of flowering branches from a single plant species. During the Old and Middle Kingdoms, formal bou-

quets became more organized, and tied together using basic methods. This development reached its pinnacle in the New Kingdom, characterized by intricate and detailed arrangement [2]. These differences underscore the significance of preserving ancient bouquets. After being unearthed, they were exposed to inadequate display environments, leading to the build-up of dust and dirt that formed a layer over the fibers. This damage is compounded by their burial in unsuitable conditions for extended periods and the absorption of moisture by the plant fibers. Additionally, the inherent properties of the plant fibers themselves contribute to the deterioration, as they decompose more quickly than other organic materials. The separation of leaves from stems and the tearing of the leaves can further damage the bouquets [3]. When the moisture content of the artifacts decreases, another aspect of damage becomes apparent: the separation of fibers due to fluctuations in relative humidity and temperature during their continuous cycle of drying and moistening. These ongoing changes ultimately lead to detachment and increased degradation of the plant-based bouquets [4]. A scaled-down model of a funerary bouquet was created, inspired by a bouquet of persea bearing Carter's number 018, JE 62725, Exhibition number at the Egyptian museum, Tahrir 1659, SR 2773, GEM 14279 [5]. The bouquet was discovered in Thebes, in the tomb of Tutankhamun, where it was pos-itioned against the southern wall in the southwest corner of the burial chamber. A context that places the bouquet within the New Kingdom (Eighteenth dynasty), emphasizing its cultural significance in ancient Egyptian funerary practices and the importance of floral arrangements in honoring the deceased. The model of this bouquet exemplifies the craftsmanship of ancient Egyptian floral arrangements, according to Hamdy (2005). The large mortuary bouquet is about 167 cm long, consisted of several leafy branches of persea (*Mimusops laurifolia*), along with a few leafy branches of the olive tree (*Olea europaea*). The components were carefully arranged on five culms of the common reed (*Phragmites australis*) and bound with strips of date palm leaflets (*Phoenix dactylifera*). Additionally, the handle of the bouquet was adorned with large leaves of persea, which were also wrapped with ribbons of date palm leaflets [6]. Due to the inherent fragility and degradation of these materials, along with the challenges associated with their treatment and consolidation, researchers are interested in focusing on methods to strengthen floral bouquets for more effective handling. In the absence of previous studies specifically targeting this issue, existing literature related to the consolidation of analogous organic materials, such as plant fibers, including papyrus, Khalifa [7] conducted an experimental study evaluating the effects of various consolidants, such as Klucel E, Klucel G, and methylcellulose on artifacts made of plant fibers. The findings demonstrated that Klucel E, at a concentration of 1% gave the most favorable results. In a study by Hamed, et al. [8] dyed cotton textiles were consolidated by adding halloysite nanoclay ($Al_2Si_2O_5(OH)_4.2H_2O$) 1%, ZnO-NPs to Klucel G 1% for enhancing the consolidation process, which improved their mechanical properties without color, morphological, and chemical changes. In another study the efficacy of incorporating nanocellulose for the consolidation of cellulose-based materials, such as fabrics, paper, textiles, and wood was documented, and the authors emphasized that nanocellulose provides significant strength and stability while forming a transparent film, making it a highly valuable alternative due to its non-toxic properties and compatibility with the original materials, particularly when compared to traditional consolidation methods [9]. When utilized for reinforcing canvas, nanocellulose has proven to be an effective and ecofriendly substitute for synthetic polymers, offering no noticeable changes to the canvas and exhibiting low penetration, which is advantageous for reversibility. Furthermore, Caruso, et al. highlighted the importance of employing reversible and non-toxic materials in cultural heritage preservation. They pointed out that biopolymers represent a viable alternative to synthetic polymers and solvents that pose risks to human health and the environment [10]. Natural biopolymers can be categorized into polysaccharides and proteins, all of which are characterized by their low cost and environmental sustainability. Adriana et al. examined the incorporation of nanomaterials into traditional wood consolidation methodologies, elucidating the benefits of various nanomaterials, including titanium dioxide, ZnO, iron oxide, copper, silver, and silica dioxide, as well as their respective application techniques [11]. Previous research reflects the growing interest in selecting materials that enhance the durability and stability of historical artifacts. Younis, et al. conducted a study on methyl cellulose (MC)–cellulose nanocrystal (CNC)–lignin bio-composites as sustainable consolidants for archaeological wood preservation. The composites were prepared via aqueous blending, and after lignin addition they provided near-complete UV protection and reduced water vapor transmission by ~40 % [12]. In a study on the strength enhancement of Klucel E with cellulose nanofibrils, the treatments not only enhanced fiber flexibility but also increased their resistance to environmental deterioration processes, offering promising potential for their use in the conservation and restoration of archaeological materials [13]. In another study by Salim, traditional chitosan, nano chitosan, and chitosan/ZnO NPs were assessed as environmentally friendly consolidants for papyrus paper [14]. Dadmohamadi, et al. also evaluated the potential of nanocellulose fibers as a consolidating agent to restore the mechanical integrity of paper [15]. Nanotechnology deals with materials at the

nanoscale, examining properties in the size range of 1-100 nm. The reduction in material size leads to unique physical and chemical properties [15]. Among various synthesis methods, green synthesis, also known as biosynthesis, is considered an environmentally friendly and efficient approach. This method utilizes living organisms and plant extracts as reducing and stabilizing agents, avoiding toxic chemicals and minimizing environmental impact. The application of biosynthesized nanoparticles in conservation offers potential benefits due to their lower toxicity and sustainable production compared to conventional physical and chemical methods [16]. This preliminary experimental study aims to evaluate the efficacy of various cellulose-based materials and nano engineered composites for their treatment and consolidation. Special focus is placed on consolidants mixed with plant-based extractives, valued for their biocompatibility and environmental sustainability. By simulating natural aging and applying these treatments, the study seeks to identify the most effective conservation materials, thereby contributing to the preservation of these culturally and historically significant floral artifacts.

2. Material and Methods

2.1. *Collecting plants*

Branches and leaves were collected from different locations in Egypt as follows: persea branches from El Nahr Garden at Gezira, Zamalek, Cairo; date palm leaflets from Edfu, Aswan governorate; and olive branches from the Orman Botanic Garden, Giza. Upon collection, all plant materials underwent a thorough cleaning process to remove dirt, dust, and any other surface contaminants. The leaves and branches were gently rinsed under running water to avoid damage to delicate tissues. After rinsing, the samples were carefully dried at ambient room temperature (approx. 22-25 °C) in a well-ventilated, dust-free environment for 48 hours to ensure complete moisture removal without inducing stress or deformation in the plant fibers, fig. (1).

Figure (1) the steps for making a copy of a bouquet; **a.** the archaeological bouquet Carter no. 18 (*After: the Griffith Institute, Univ. of Oxford*), **b.** leaves on persea twigs, which were used as one of the main plant components, **c.** leaves on olive twigs, **d.** & **e.** common reed culms after cleaning and leaf removal, **f.** date palm fronds after cleaning and cutting, **g.- j.** forming the bouquet step-by-step, **k.** fully assembled bouquet, **l.** the new bouquet after aging.

2.2. *Accelerated thermal aging*

Artificial aging protocols were applied to simulate the natural degradation processes experienced by ancient floral artifacts over time using BTC Thermal aging oven, Biotech Company for medical & laboratory equipment, Serial Number: BT 2020, Metal Research and Development Center in Tebin, Helwan, Egypt. The thermal aging oven was used to thermally age the model bouquets and leaves, to simulate the dryness of the ancient plant materials found on excavation sites and in museum collections. In the absence of a specific standardized method for the thermal aging of plant fibers, the standards used for paper made from wood pulp was adapted. The aging process was maintained at a stable temperature of 90 °C for 120 h., and was carried out before the application of trea-tment materials to the different plant materials under study, ensuring that the evaluation of their performance under accelerated aging conditions was solely based on the effects of heat [17,18].

2.3. *Treatment materials and procedures*

In a referenced study, nanostructured composites prepared by adding Halloysite nano-clay and ZnO NPs separately to Klucel G 1% solution at ratios of 0.5 and 1 oven-dry wt.% based on weight of dry Klucel G were used to treat cotton textiles [8]. Klucel E (Hydroxypropyl Cellulose, HPC), a non-ionic cellulose ether, has been widely used in the field of organic consolidation material due to its high effectiveness in improving the structural stability of such materials [19,20]. It is water-soluble at temperatures below 38 °C but becomes insoluble above 40 °C. It is also soluble in several polar organic solvents, such as ethyl alcohol and 95% isopropyl alcohol. Its superior performance was confirmed in a previous comparative study that evaluated Klucel E, Klucel G, and methyl cellulose, applied to five types of plant fibers: *Phoenix dactylifera*, *Hyphaene thebaica*, *Cyperus papyrus*, *Desmostachya bipinnata*, and *Juncus acutus* [7]. In the past decade, natural extracts have gained attention for their potential applications in inhibiting mould growth on organic materials such as wood. For this experimental study three extracts were separately prepared from 10 grams of the leaves of the persea plant, 10 grams of olive leaves, and 10 grams of date palm leaflets, each mixed with 90 mm. of acetone and 10 mm. of distilled water [21,22]. The precipitate of each extract was filtered and each plant extract was mixed with Klucel E (1 %) for treating the corresponding leaves, i.e. persea extract for persea leaves, olive extract for olive leaves and palm extract for palm leaflets. Two different nanoparticles (NPs) were chosen for this experimental study. Zinc oxide (ZnO NPs), prepared by green synthesis using extract of *Ocimum basilicum* [23, 24] and magnesium oxide (MgO NPs) prepared by green synthesis using *Hyoscyamus muticus* leaf extract

based on the aforementioned studies [16]. ZnO NPs showed good photo catalysis and antibacterial activity and MgO NPs had an inhibitory effect on the growth and the production of α-amylase of both *A. niger* and *A. ochraceous*. Either ZnO NPs or MgO NPs were added to the aforementioned mixtures of Klucel E and plant extracts using the ultrasonication technique. Sonication using a 750 VCX Cell-Vibra Sonics device (750 watts, 50 Hz ± 20 kHz) significantly accelerated the dissolution of both ZnO NPs and MgO NPs. The process was completed in 15 minutes for ZnO NPs and 12 minutes for MgO NPs respectively. For the evaluation of the aforementioned treatment materials four leaves from each of the three plant leaves under study were prepared for consolidation. Only half of each leaf was covered with the polymer lengthwise by brush application, while the other half remained untreated and was used as a control sample during investigation and analysis. The first leaf of each plant was covered with a layer of Klucel E, the second leaf was treated using a mixture of the plant extract and Klucel E, the third leaf was treated with a mixture of Klucel E, plant extract and ZnO NPs, while the last leaf was treated with a mixture of Klucel E, plant extract and MgO NPs.

2.4. *Evaluation methods*

The effectiveness of the treatments was evaluated through a comprehensive set of analytical techniques, including visual inspection, digital microscopy (USB), colorimetric change analysis, pH measurement, contact angle assessment, and ATR-FTIR spectroscopy. This multi-method evaluation allowed for detailed monitoring of both physical and chemical changes caused by aging and consolidation treatments, providing critical insights into the performance of each consolidate.

2.4.1. Visual assessment using USB

Critical visual assessment was used to evaluate the effectiveness of treatments and give an initial opinion on the treatment processes. A digital camera Nikon D-7500 was used to systematically document all phases of the experimental study, ensuring precise visual records of the procedural steps and a LCD Digital Microscope at the Royal Carriage museum in Cairo was utilized for observing surface changes (Shenzhen Super Eyes Co., Ltd., Guangdong, China with a magnification power of up to 1000X).

2.4.2. Attenuated total reflectance-fourier transform infrared spectroscopy

A Bruker FTIR Vertex 70, at the Projects Sector of the Scientific Research Department at the Ministry of Antiquities (Cairo) was used for analyzing the treated leaf surfaces. The samples were analyzed in the spectral range of 400-4000 cm^{-1} using the Attenuated Total Reflectance (ATR) unit, which requires no prior preparation and minimizes damage to the samples.

2.5. *Measurements*

2.5.1. pH measurement

The determination of pH in cold aqueous extracts of plant samples was conducted following ISO 6588-1:2021-11 using calibrated pH electrodes [25]. The pH value of the plant extracts was measured using Adwa AD1030 pH meter, which is a waterproof temperature pocket tester equipped with a replaceable probe. The samples, weighing 0.5 grams each, were soaked in 40 milliliters of distilled water at room temperature for one hour.

2.5.2. Change *of* color

The color changes resulting from the aged plant samples were measured and compared to the control samples using the R3100 Optimatch spectrophotometer manufactured by SDL. To express the color changes, the CIE LAB color system was utilized, allowing for the measurement of white (W) and yellow (Y) color values. The total color change was calculated using the formula: $\Delta E = \sqrt{((\Delta L^*)^2 + (\Delta a^*)^2 + (\Delta b^*)^2)}$ [26].

2.5.3. *Contact angle measurement (wettability)*

The contact angle of control and treated samples were determined according to El-Bisi et al. [27] and ASTM D724-99 [28]. This test was conducted using a Compact Video Microscope (CVM) manufactured by SDL-UK. The average water drop volume applied to the surface of the tested samples was 2.5 µL. This test was carried out at a room temperature of 22 ±1 °C and relative humidity 65 ±5%.

3. Results

The study examined the effect of various consolidation materials on the three different leaves that formed the model plant bouquet. Klucel E polymer, Klucel E with plant extract, Klucel E+plant extract+ ZnO NPs and Klucel E+plant extract+MgO NPs mixtures were applied, as shown in fig. (2) The results of these tre-atments were evaluated as follows:

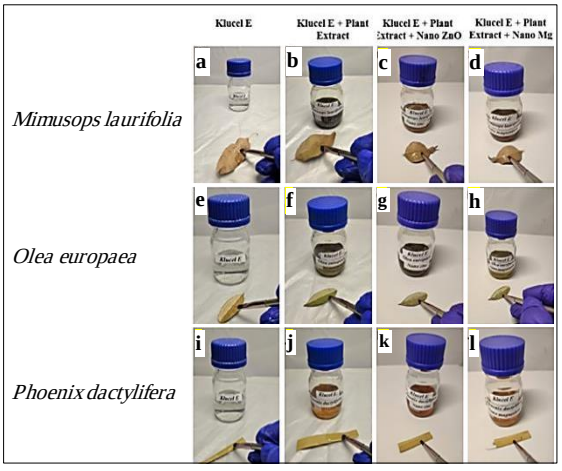

Figure (2) the application of consolidation materials on the plants under study

3.1. *Visual examination*

Visual examination of the samples revealed several changes in the surface appearance of the studied plants. Acceptable color changes were observed with the naked eye in most samples; however, a noticeable gloss was observed on the surface of samples treated with Klucel E, figs. (3,4,5-a). Additionally, brown-colored residues appeared on sample surfaces treated with ZnO NPs, figs. (3,4,5-c) and the consolidated areas appeared less dry in most samples, while samples treated with MgO NPs exhibited the least color change, figs. (3,4,5-d) except for those treated with Klucel E+plant extract, figs. (3,4,5-b) which did not exhibit any noticeable change to the naked eye.

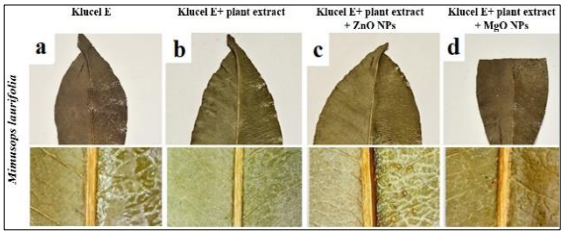

Figure (3) photographic documentation and USB digital microscope examination of *M. laurifolia* before and after applying the consolidation materials.

3.2. *USB microscopic examination*

After the initial visual examination, a digital microscope was employed to further confirm the observed changes in the samples. The result of Klucel E on persea leaf showed a slight gloss and minor color change, fig. (4-a). Conversely, no noticeable alterations were detected under the microscope when Klucel E was combined with the plant extract, fig. (4-b). A thin glossy layer appeared on the surface when Klucel E+plant extract+ZnO NPs was applied, showing a slightly more pronounced effect than Klucel E alone, fig. (4-c). Meanwhile, the formulation of Klucel E+plant extract+MgO NPs provided improved results compared to ZnO NPs but exhibited less change than Klucel E+plant extract, fig. (4-a). For olive tree leaves, the application of Klucel E caused noticeable surface modifications, as observed under the digital microscope, fig. (5-a), and when Klucel E was combined with olive extract, the surface changes were less pronounced compared to Klucel E alone, fig. (5-b). However, the application of the nanoparticles, both Zn and Mg, to Klucel E and plant extract mixtures resulted in more pronounced surface changes, fig. (5-c). As for date palm fronds, fig. (5-d), no significant surface differences were observed after applying the polymer and polymer mixtures, except for the mixture com-posed of Klucel E+plant extract+ ZnO NPs, which resulted in a noticeable change in the consolidated area.

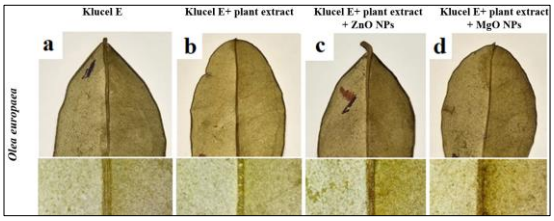

Figure (4) photographic documentation and USB digital microscope examination of *O. europaea* before and after applying the consolidation materials.

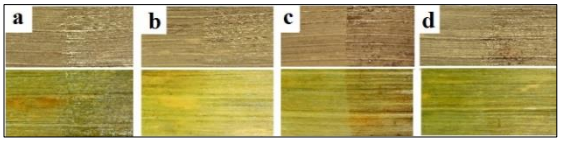

Figure (5) photographic documentation and USB digital microscope examination of *P. dactylifera* before and after applying the consolidation materials.

3.3. *pH measurement*

The pH values of all the studied plant samples were below 6, while the pH value of Klucel E was 8.6. When the plant extract was mixed with Klucel E and either MgO NPs or ZnO NPs, all pH values changed slightly ranging between 6.6 and 7.5, fig. (6):

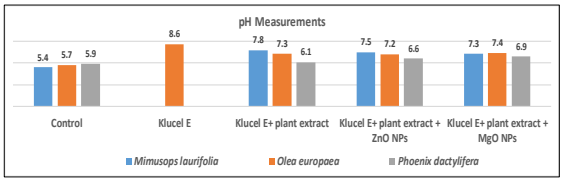

Figure (6) pH of control and treated samples

3.4. *Color change measurements*

The color parameters L, a, and b of the treated samples were measured before and after treatment, and total color differences (ΔE) were calculated, fig. (7). The findings are summarized as follows: For persea, none of the treated samples exhibited noticeable color changes to the naked eye, with all ΔE values being below 3. The treatment with Klucel E+persea extract showed the best result, with a ΔE value of 1.32. This was followed by Klucel E treatment alone on persea leaves, which had a ΔE of 1.45. The third-best result came from the combination of Klucel E+persea extrac+ MgO NPs, with a ΔE value of 1.74. The highest color change recorded was in the sample treated with Klucel E+persea extract+ZnO NPs, which had a ΔE value of 2.29. In the case of olive tree leaves, all treated samples showed noticeable color changes, with ΔE values exceeding 3. The best result came from the treatment of Klucel E+olive extract, which had a ΔE value of 4.60. This was followed by the combination of Klucel E+olive extract+MgO NPs, with a ΔE value of 5.45. The third-best result was seen with the treatment of Klucel E+olives extract+ ZnO NPs, which had a ΔE of 5.86. The highest color change was observed with the application of

Klucel E alone on olive leaves, which resulted in a ΔE value of 8.14. For date palm fronds, three of the treated samples did not show noticeable color changes to the naked eye, with ΔE values remaining below 3. The best result was seen in the sample treated with Klucel E+date palm extract, which showed no visible color change, resulting in a ΔE of 0.25. The application of Klucel E alone on date palm fronds resulted in a ΔE of 2.17, while the combination of Klucel E+ date palm extract+ MgO NPs came third, with a ΔE of 2.97. The most significant color change occurred with the treatment of Klucel E+date palm extract+ ZnO NPs, which resulted in a noticeable color difference with a ΔE value of 4.13.

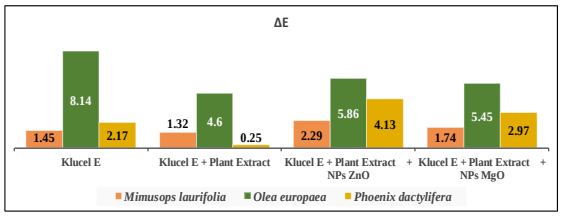

Figure (7) total color difference value (ΔE) of the consolidation materials on the persea, olive, and date palm leaves

3.5. *Contact angle measurement*

The contact angle of water droplets on the control samples, which had been exposed to accelerated ageing to simulate the studied archaeological plants, ranged between 123º and 134º. After applying the treatments, the contact angle measurements at 1.19 minutes for all persea leaves gave different measurements. In the samples treated with Klucel E the contact angle ranged between 96.91º-83.00º, while persea leaves treated with plant extract+Klucel E recorded a contact angle ranging from 48.84º:38.78º. In the sample treated with ZnO NPs the contact angle ranged from 74.63º-73.34º, while the contact angle in the sample treated with MgO NPs was around 38.21º-38.15º. In the olive plant samples, the time that elapsed before measuring the contact angle varied from one treatment to the other. In the sample treated with Klucel E the contact angle ranged between 88.40º-83.11º at 2.38 minutes, while the samples treated with Klucel E and plant extract measured 47.12º-46.70º at 9.45 minutes. Olive samples treated with ZnO NPs recorded a contact angle between 129.68º-93.57º at 4.9 minutes, while those treated with MgO NPs ranged from 37.21º-37.06º at 33.34 minutes. Similar to persea samples the initial measurement of all date palm samples was at 1.19 minutes. The sample treated with Klucel E exhibited a contact angle of 65.55º-64.11º, while the sample treated with Klucel + palm extract exhibited a contact angle of 57.88º-53.27º. The contact angle of the sample treated with ZnO NPs was between 66.24º-65.77º, while that of the MgO NPs was between 84.86º-81.48º. These results indicate that all treated samples underwent a change and became more water-absorbent (hydrophilic), even though the ranges varied between the olive leaf samples and the remaining two types, figs. (8 & 9).

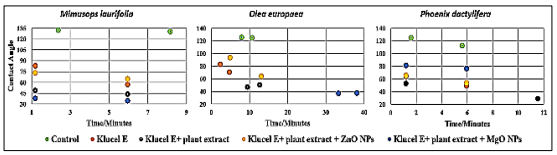

Figure (8) scatter plot showing a different trend of contact angle measurements in the treated olive leaves after several minutes compared to the persea and date palm leaves.

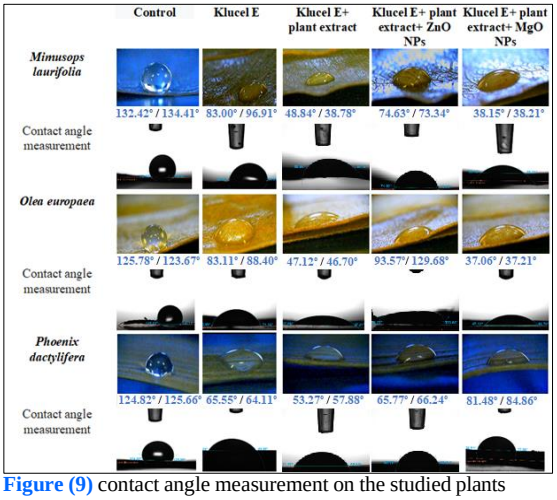

Figure (9) contact angle measurement on the studied plants

3.6. *ATR-FTIR results*

Each plant leaf exhibited distinct behavior based on its functional groups. Although cellulose and hemicellulose are the primary components commonly found in all plants, lignin was notably abundant in the olive plant compared to the other species under study. In contrast, lignin was absent in the aged persea plant and appeared only in the form of small peak after treatment, while it was detected in very low concentrations in the date palm leaf. The following sections will discuss the main functional groups identified in the various samples, as revealed by ATR-FTIR analysis:

3.6.1. Persea leaves

FTIR spectra showed significant changes in persea leaves before and after treatment, tab. (1). In the control sample the broad OH stretching band related to cellulose, hemicellulose, and lignin appeared at 3424 cm^{-1} with an intensity of 0.010. After treatment with Klucel E, this band shifted to 3411 cm^{-1} with a higher intensity of 0.026, indicating stronger hydrogen bonding or more exposed OH groups. The sample treated with Klucel E and plant extracts showed a further shift to 3353 cm^{-1} and increased intensity of 0.028. With the addition of ZnO NPs the band appeared at 3396 cm^{-1} with an intensity of 0.022,

whereas the addition of MgO NPs exhibited a shift to 3371 cm^{-1} and the highest intensity of 0.030 compared to the other treatments The peaks near 2900 cm^{-1}, related to C–H stretching in aliphatic groups, also showed intensity variations. In the control sample this peak was at 2917 cm^{-1} with an intensity of 0.084. After treatment the intensities decreased: Klucel E at 2917 cm^{-1} (0.061), Klucel E+plant extracts at 2920 cm^{-1} (0.045), while the intensity of the peak at 2920 cm^{-1} measured (0.034) after the addition of ZnO NPs and at 2918 cm^{-1} (0.036) after the addition of MgO NPs [29].

Table (1) the wavenumbers in cm-1 of FTIR spectra of the persea leaves

Mimusops laurifolia	O-H Stretching	C-H Stretching	H-O-H Bending	CH_2-CH_3 Bending	C-O-C Stretching
Control	3424	2917	---	1460	1028
Klucel E	3411	2917	1640	1452	1045
Klucel E+ plant extract	3353	2920	1611	1453	1045
Klucel E+ plant extract+ ZnO NPs	3396	2920	1612	1453	1047
Klucel E+ plant extract+ MgO NPs	3371	2918	1612	1453	1046

The 1505-1511 cm^{-1} for C=C stretching vibration in lignin aromatic skeletal did not appear initially, but it was detected after treatment with Klucel as well as Klucel combined with the plant extract at 1515 cm^{-1}. It was observed at 1513 cm^{-1} when treated with Klucel E and the plant extract enhanced with ZnO NPs, and at 1510 cm^{-1} with the treatment using MgO NPs added to Klucel and the plant extract. From the results the H-O-H absorption group in all treated samples was detected, in contrast to the aged control sample, where this group was not recognized. The peaks observed at 1046 and 1453 cm^{-1} correspond to C-O-C stretching and CH_2 bending. Though many bands did not change significantly, minor shifts in wave-numbers and intensity variations were noticed. These changes highlight the structural features of the persea leaves post-treatment, as confirmed by the contact angle measurements.

3.6.2. Olive leaves

The OH stretching band in cellulose, hemicellulose, and lignin of the aged plant appeared at 3428 cm^{-1} with an intensity of 0.019. The treated samples of the olive leaf showed an increased intensity in the OH stretching band in cellulose, hemicellulose, and lignin, tab. (2) The spectra of the plant treated with Klucel E appeared at 3403 cm^{-1} with an intensity of 0.031, the plant treated with Klucel E+ plant extracts appeared at 3400 cm^{-1} with an intensity of 0.055, and the plant treated with Klucel E+plant extracts+ZnO NPs appeared at 3401 cm^{-1} with an intensity of 0.061, which was the highest intensity among the treated plants [30]. The spectrum of the plant treated with Klucel E+plant extracts+MgO NPs showed the highest OH band stretching at 3398 cm^{-1} with an intensity of 0.058. After treatment, this band showed a significant increase in intensity and width shifting to 3398 cm^{-1}. The smaller bands near 2900 cm^{-1}, which are related to the stretching of C–H in the aliphatic region were observed at 2920 cm^{-1} with an intensity of 0.061, the plant treated with Klucel E appeared at 2919 cm^{-1} with an intensity of 0.077, and the leaves treated with Klucel E+plant extracts appeared at 2919 cm^{-1} with an intensity of 0.083. The spectrum of the plant treated with Klucel E+plant extracts+ZnO NPs appeared at 2918 cm^{-1} with an intensity of 0.083. The spectrum of the plant treated with Klucel E+plant extracts+MgO NPs appeared at 2918 cm^{-1} with an intensity of 0.076. The bands at 1652 cm^{-1} that correspond to the vibrations of C–O, barely changed in their intensities, except for the slight increase in the sample treated with Klucel E.

Table (2) the wavenumbers in cm^{-1} of the FTIR spectra of olive leaves

Olea europaea	O-H Stretching	C-H Stretching	C=O Stretching	C-O Bending	N–H Stretching	CH2-CH3 Bending	C-N Stretching
Control	3422	2920	1729	1652	1515	1375	1031
Klucel E	3403	2919	1729	1650	1515	1373	1046
Klucel E+ plant extract	3400	2919	1732	1645	1514	1373	1047
Klucel E+ plant extract+ ZnO NPs	3401	2918	1732	1632	1513	1373	1047
Klucel E+ plant extract+ MgO NPs	3398	2918	1733	1631	1513	1373	1046

Olive leave extract contains organic functional groups such as alkanes, aromatic compounds, and amide linkages from proteins and amines. Amide II or N–H stretching at 1518.81 and 1521.75 cm^{-1}, and C–N vibrations at 1018.58 and 1021.34 cm^{-1}, which are characteristic of amines were previously recorded [31]. The band at 1527 cm^{-1}, which is characteristic of amide II, is attributed to the N–H stretching vibrations in the amide bond. The C=C stretching vibration in lignin aromatic skeletal group appeared at 1515 cm^{-1} in the control olive leaf and in the leaf treated with Klucel E. In the leaf treated with Klucel E+ plant extract it appeared at 1514 cm^{-1}, while in the leaves treated with either Klucel E+plant extract+ ZnO NPs or Klucel E+plant extract+Mg NPs it appeared at 1513 cm^{-1}. Meanwhile, the band at 1375 cm^{-1} is attributed to methylene scissoring vibrations originating from proteins. The strong band at 1076 cm^{-1} can be attributed to C–N stretching vibrations of aliphatic amines or C–OH vibrations of proteins in olive leaves. This indicates the presence of carbonyl (-C=O), hydroxyl (-OH), and amine (N–H) groups in the extract of olive leaves [32].

3.6.3. Date palm leaflets

FTIR spectra showed some changes in date palm leaflets before and after treatment, tab. (3). The OH stretching band in cellulose, hemicellulose, and lignin of the aged plant appeared at 3327 cm^{-1} with an intensity of 0.025. The treated samples of date palm leaflets showed an increased intensity in the OH stretching band in cellulose, hemicellulose, and lignin. The spectrum of the plant treated with Klucel E

showed the lowest OH stretching band at 3428 cm^{-1} with an intensity of 0.011. The spectrum of the plant treated with Klucel E+plant extracts appeared at 3397 cm^{-1} with an intensity of 0.049. The spectrum of the plant treated with Klucel E+plant extracts+ ZnO NPs appeared at 3409 cm^{-1} with an intensity of 0.052. The spectrum of the plant treated with Klucel E+ plant extracts+MgO NPs appeared at 3399 cm^{-1} with an intensity of 0.052 [33]. The smaller bands around 2900 cm^{-1} attributed to the stretching of C–H in the aliphatic group appeared in the aged plant at 2917 cm^{-1} with an intensity of 0.125, while the intensity decreased in all treated plants. The spectrum of the plant treated with Klucel E appeared at 2916 cm^{-1} with an intensity of 0.023, and the spectrum of the plant treated with Klucel E+plant extracts appeared at 2917 cm^{-1} with an intensity of 0.080. The spectrum of the plant treated with Klucel E+ plant extracts+ ZnO NPs appeared at 2917 cm^{-1} with an intensity of 0.070. The spectrum of the plant treated with Klucel E+plant extracts+MgO NPs appeared at 2917 cm^{-1} with an intensity of 0.048.

Table (3) the wavenumbers in cm^{-1} of FTIR spectra of date palm leaflets

Phoenix dactylifera	O-H Stretching	C-H Stretching	C-O/ C-C/C=C Stretching	C-O/C-C/C=C Stretching	C-O/C-H Stretching
Control	3422	2920	1651	1460	1031
Klucel E	3403	2919	1641	1454	1047
Klucel E+ plant extract	3400	2919	1647	1454	1047
Klucel E+ plant extract+ ZnO NPs	3401	2918	1640	1454	1047
Klucel E+ plant extract+ MgO NPs	3398	2918	1642	1454	1047

According to several references it was very difficult to assign the band detected at 1516 cm^{-1} in the aged date palm leaf to a specific functional group. This band is usually assigned to the aromatic ring of lignin, and in literature this fact is verified by extracting lignin from *Phoenix dactylifera* fronds during lignocellulosic biomass production [34]. However, Mahdi et al. noted that amide II is produced by N–H bending vibrations and C-N stretching vibrations in the spectra of date palm leaves between 1520 and 1515 cm^{-1}. They also mentioned that N–H bending in the plane, C-N stretching and C-H in plane bending of phenyl rings (tyrosine) generated the bands in this location (amide II) [35]. Whether this band is related to lignin or amide, will not be discussed here, but it is worthy to point out that it was recorded in the aged sample. After treatment its intensity was smaller, but it remained present. There was a noticeable rise in the bands near 1414 and 1327 cm^{-1}, which are attributed to CH_2 scissoring vibrations and OH bending, respectively. After treatment, this band showed a significant increase in strength and vibration intensity for OH stretching. The bands at 1651 and 1454 cm^{-1}, which relate to C–O, C-C, C=C of the aromatics were all present in the samples [36]. The band at 1047 cm^{-1} indicates the presence of C−H and C−O stretching in alcohols, carboxylic acids, esters, and ethers. Stretching and CH_2 bending, respectively. Furthermore, carbonyl groups that may have formed due to additional oxidation of C–OH groups in carbohydrates were reduced. In many bands of the spectrum, only slight changes in wavelength occurred. These differences are attributed to variations in absorption strength at specific wavelengths, highlighting the structural features of the date palm leaflets after treatment, as shown in fig (10).

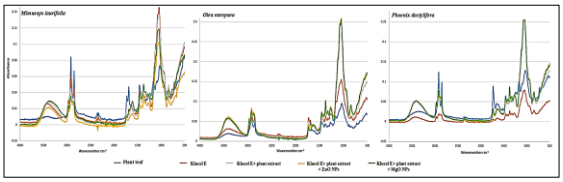

Figure (10) ATR-FTIR spectra of the treated plant leaves

4. Discussion

Previous studies on chemically treated plant fibers, such as hemp, cotton fibers, and flax, have shown a reduction in their hydrophilicity, enhancing moisture resistance and improving thermal stability [37]. Similarly, consolidation material enhanced with nanomaterials, such as ZnO NPs, demonstrated promising results in preserving historical organic materials like paper and improving their mechanical properties [38]. Other studies have demonstrated that the application of Klucel E or Klucel G in combination with nano-additives significantly improved the mechanical properties of plant-based fibers commonly found in archaeological and heritage objects [39,40]. In this study contact angle measurements indicated that no significant water absorption occurred in the aged samples, reflecting their high hydrophobicity, in contrast to the treated samples that exhibited an increased degree of hydrophilicity. Treated plant fibers demonstrated enhanced flexibility, resulting in an improved surface appearance, which is in agreement with the fact that natural treatments and nanomaterials restore the plant's moisture content, indicating efficient absorption of the treatment materials and their uniform distribution within the fiber structure [41]. Upon examining the samples with a USB microscope, the cell wall became distinctly visible after the consolidation process, in contrast to its previous state. This was particularly evident when Klucel E was applied to the three plant samples. However, a noticeable surface gloss was observed after application. When Klucel E was combined with the extract of each plant, the undesired gloss disappeared, while the distinctive surface lines of the plant leaf remained clearly visible, indicating the plant's recovery of its moisture content. Another clear example of brittleness, fragility and distinctive surface lines of the plant leaf was observed indicating fiber dryness in the date palm fibres prior treatment, in contrast to the fibres treated with

the strengthening materials under study. The incorporation of nanomaterials alongside Klucel E and the plant extracts further enhanced the consolidation process. The effectiveness of the treatments is contingent on the fibres type and the specific formulation used. For olive tree leaves, the treatment with Klucel E and nanoparticles resulted in a noticeable change in surface morphology. Significant variations were also observed depending on the type of nanomaterial used. Specifically, the application of ZnO NPs on persea resulted in the reappearance of surface gloss, whereas MgO NPs maintained the distinctive surface lines of the plant leaf without any gloss. The pH measurement results indicated some significant effects on plants during the conservation process. Klucel E, being alkaline, raised the pH to 8.6, while plant control such as persea, olive leaves and date palm fibres lowered the pH to values ranging from 5.4; 5.9, reflecting the acidic nature of our study organic extracts. This suggests that the interaction between these extracts and Klucel E can have diverse effects on the stability of the plants. Also, the addition of nanoparticles like ZnO and MgO, while Klucel E and plant extract contributed to providing greater protection. This interaction between alkaline and acidic components highlights the importance of selecting well-balanced components to ensure effective conservation and maintain the stability of paper materials [42,43]. The study revealed varying color changes (ΔE values) for persea, olive, and date palm leaflets, reflecting the impact of different treatments on the plants' preservation. For persea, the color changes were minimal, with all ΔE values below 3, indicating that the treatments had a subtle effect on the leaves. The combination of Klucel E and persea extract showed the best result (ΔE= 1.32), preserving the original color effectively. In contrast, olive leaves exhibited significant color changes, especially with the inclusion of Klucel E and nanoparticles, however, the highest ΔE value reached 8.14 with Klucel E alone. This suggests that olive leaves are more sensitive to the treatments, and caution is needed when applying certain combinations. Date palm leaflets showed greater stability, with minimal color changes (ΔE< 3) in most treatments, except when ZnO NPs were added, which resulted in the most noticeable color change (ΔE= 4.13). These results emphasize the varying levels of sensitivity of different plant types when applying the same treatment procedures. While persea and date palm leaflets appear to show minimal to moderate color changes, olive leaves, with their distinct chemical composition, are more reactive to treatments, particularly those involving Klucel E and nanoparticles. The observed higher ΔE values for olive leaves suggest that a more cautious approach should be taken when treating these plants, possibly involving a reduction in the concentration of nano-particles or alternative formulations that minimize color alteration. All the studied plants demonstrated their ability to absorb water. Contact angle measurements indicated that the plant's water absorption capacity increased, except for the plant treated with a mixture of Klucel E and plant extract. This means that the dry, brittle, and fragile leaves restored their water content, thus con-tributing to their flexibility. This, in turn, facilitates the treatment and maintenance processes for these rare and highly vulnerable artifacts. The above-mentioned results are consistent with the ATR-FTIR analysis of the treated leaves, which revealed certain changes in the chemical composition of leaves from persea, olive tree, and date palm. All the treated samples—persea, olive, and date palm leaves—showed an increased intensity in the (OH) hydroxyl band of cellulose, hemicellulose, and lignin. This corresponds with the functional groups present in the ZnO nanoparticles, as confirmed by FTIR, indicating a main absorption band at 3418 cm^{-1}, which represents the O–H stretching vibration of water molecules [23]. It is also in agreement with the FTIR spectrum of MgO nano-particles (MgO NPs), which displayed a broad absorption band centered at 3421 cm^{-1}, corresponding to O–H stretching vibrations in alcohol groups [44]. Furthermore, the spectrum of the treated plant leaves showed increased intensity of the bands at 1416 and 1326 cm^{-1} across all types of leaves after treatment, indicating changes in chemical vibrations such as CH_2 scissoring and OH bending. In addition, the O–H stretching vibration peak increased in intensity after treatment, shifting from 3428 cm^{-1} to 3412 cm^{-1}. This shift in wavenumber reflects stronger hydrogen bonding within the fiber's molecular structure, contributing to enhanced structural stability and making the leaves more resistant to degradation. Moreover, the reduction of carbonyl groups, which may have formed due to further oxidation of C–OH groups in carbohydrates, indicates that the treatment helped to limit oxidation, thus improving fiber longevity and resistance to decomposition. In the case of olive tree leaves, an increase in peak intensities at 1645 cm^{-1} (CH groups) and 1514 cm^{-1} (C=C) was observed, suggesting changes in lignin structure. This implies that the treatment affected lignin content, enhancing the structural properties of the fibers through interaction with lignin. Additionally, the ZnO composite absorption band appeared between 400 and 560 cm^{-1} [23] in all three plant samples studied. Likewise, the FTIR spectrum of the synthesized MgO NPs appeared in the range of 400 to 447 cm^{-1}, confirming the presence of MgO NPs in all three plant samples under investigation. Natural treatments can significantly enhance the surface properties and characteristics of plant fibers. Various tests and analyses conducted on the selected treated plant samples in this study have confirmed that they have transitioned from being dry and brittle to more flexible. Most probably

the moisture content of the plants has been restored, as evidenced by contact angle measurements, which indicated a significant increase in water absorption capacity. Additionally, ATR-FTIR analysis revealed an increase in the intensity of the hydroxyl (-OH) functional group, facilitating further conservation and restoration processes, such as bundling branches together or reconstructing damaged plant-based artifacts.

5. Conclusion

Klucel E combined with plant extracts and nanoparticles (NPs) was chosen for this preliminary study to treat three types of leaves used in archaeological bouquets and garlands. Visual examination revealed significant changes in the surface properties of the treated fibers, including improved flexibility and reduced brittleness—two crucial factors for preserving fragile plant materials. The treatment results were further enhanced by incorporating nanoparticles such as magnesium oxide and zinc oxide, particularly in olive fibers, which exhibited notable surface modifications. Olive leaves exhibited significant color changes, especially when nanoparticles were added, highlighting the need for cautious application to prevent noticeable alterations in this plant material. Date palm leaflets and persea plant fibers responded more effectively to the treatment, suggesting that green materials are suitable for this type of fiber. The study also observed minor to moderate color changes in persea and date palm leaflets, indicating that most of the studied materials yielded similar results. The pH measurement results showed that various plant extracts and nano particles contribute to creating a protective natural environment, enhancing the preservation process. These findings align with previous research confirming the role of nano particles in improving the chemical stability of plant materials. Overall, this study underscores the potential of using plant-based extracts and nanoparticles as effective conservation treatments for the preservation of plant-derived materials commonly found in cultural heritage objects. Nevertheless, further research is required to evaluate the long-term stability and compatibility of these treatments to ensure their reliability in safeguarding irreplaceable archaeological plant fibers for future generations.

References

[1] Atallah, M., Tolba, M., Hamdy, R., et al. (2022). Phyto-religious symbolism in the funerary banquet scene of the tomb of Sennedjem (TT1) at Deir el-Medina. *J. of the Faculty of Archaeology*. 11: 227-245.

[2] Fahmy, A., Allué, J. & Hamdy, R. (2010). A deposit of floral and vegetative bouquets at Dra Abu el-Naga (TT 11). *BIFAO*. 110: 73-89.

[3] Wills, B. & Hacke, M. (2010). Ancient Egyptian basketry: Investigation, conservation and colour. In: Dawson, J., Rozeik, C. & Wright, M. (eds), *Decorated Surfaces on Ancient Egyptian Objects: Technology, Deterioration & Conservation.* Arc-hetype Pub., London, pp.87-95.

[4] Hegazy, T. (2005). *The scientific basis for the treatment and conservation of archaeological discoveries at excavation sites*, SCA Press, Ministry of Culture, Egypt (in Arabic).

[5] Newberry, P. (1927). *Scarabs: An introduction to the study of Egyptian seals and signet rings*. Archibald Constable & Co, London.

[6] Hamdy, R. (2005). *Documentary study of floral bouquets and garlands in ancient Egypt*. Lap Lambert Academic Pub., Saarbrücken, Germany.

[7] Khalifa, N. G. (2021). *Experimental study to evaluate some consolidation materials on baskets made from plant fibers, with application on one of the selected objects,* MA., Conservation dept., Faculty of Archaeology, Cairo Univ., Egypt (in Arabic).

[8] Hamed, S. Abouzeid, D., Sabry, W., et al., (2026). Evaluation of hydroxypropyl cellulose nanocomposites in consolidation of dyed archaeological and historical cotton textiles, *J. of Cultural Heritage*. 78: 248-255.

[9] Spagnuolo, L., D'Orsi, R. & Operamolla, A. (2022). Nanocellulose for paper and textile coating: The importance of surface chemistry. *ChemPlus-Chem*. 87 (8), doi: 10.1002/cplu.202200204.

[10] Caruso, M., D'Agostino, G., Milioto, S., et al. (2023). A review on biopolymer-based treatments for consolidation and surface protection of cultural heritage materials. *J. of Materials Science*. 58 (32): 12954-12975.

[11] Trăistaru, A., Sandu, I-C-A., Timar, M., et al. (2013). SEM-EDX, water absorption, and wetting capability studies on evaluation of the influence of nano-zinc oxide as additive to Paraloid B72 solutions used for wooden artifacts consolidation. *Microscopy Research & Technique*, 76 (2): 209-221.

[12] Younis, O., Trifol, J., Baniasadi, H., et al. (2025). A ternary methyl-cellulose/cellulose nanocrystal/lignin composite for archaeological wood consolidation: Mechanical reinforcement and aging simulation, *Int. J. of Biological Macromolecules*, 332 (2), doi: 10.1016/j.ijbiomac.2025.148725

[13] Younis, O., El Hadidi, N., Darwish, S., et al. (2023). Preliminary study on the strength enhancement of Klucel E with cellulose nanofibrils (CNFs) for the conservation of wooden artifacts. *J. of Cultural Heritage*. 60: 41-49.

[14] Salim, E., Mohamed, W. & Sadek, R. (2024). Evaluation of the efficiency of traditional chitosan, nano chitosan and chitosan nanocomposites for consolidating aged papyrus paper. *Pigment & Resin Technology*. 53 (3): 273-282.

[15] Dadmohamadi, K., Achachluei, M. & Jafari, M. (2023). Consolidation of the paper works with cellulose nanofibers. *Int. J. of Materials Science & Applications*. 12 (1): 8-14.

[16] Galal, M., Abdelsadek, M., El-Dawy, E., et al. (2022). Green synthesis of magnesium oxide nanoparticles and assessing the effect on fungal

growth and metabolism of Aspergillus species under optimum temperatures. *SVU J. of Agricultural Sciences*. 4 (3): 243-254.

[17] Salem, M., Zidan, Y., Mansour, M., et al. (2016). Antifungal activities of two essential oils used in the treatment of three commercial woods deteriorated by five common mold fungi. *Int. Biodeter. & Biodegr*. 106: 88-96.

[18] Gawish, M. (2024). *Experimental studies to assess funori and its derivative and its applications in the treatment of cellulose substrates manuscripts (physical and chemical)*, MA., Institute of Graduate Studies in Papyrology, Epigraphy, and Conservation Arts, Ain Shams Univ., Egypt (in Arabic).

[19] Abo-Elmaaref M., Marouf M., Mohamed, W., et al. (2023). Antifungal and consolidation properties of linen textiles treated with silver nanoparticles loaded on hydroxypropyl cellulose polymer. *Heritage Science*. 11 (120), doi: 10. 1186/s4049 4-023-00964-x

[20] Ramírez-Calderón, A. (2018). *Conservation of charred archaeological textiles: Consolidation treatments and long-term preservation strategies*, MA., HES-SO, Haute École Arc Conservation-restauration, Neuchâtel, Switzerland.

[21] El-Abeid, S., Mosa, M., El-Tabakh, M., et al. (2024). Antifungal activity of copper oxide nano-particles derived from Zizyphus spina leaf extract against Fusarium root rot disease in tomato plants. *J. of Nanobiotechnology*. 22 (1), doi: 10. 1186/s12951-024-02307-9.

[22] Nagar, N. & Devra, V. (2018). Green synthesis and characterization of copper nanoparticles using Azadirachta indica leaves. *Materials Chemistry & Physics*. 213: 44-51.

[23] Hussein, S., Fouad, W., Wasly, H., et al. (2023). Zinc oxide nanoparticles: Green synthesis, characterization, photocatalysis, and antibacterial activity. *Egyptian J. of Physics*. 51: 57-71.

[24] Pillai, A., Sivasankarapillai, V., Rahdar, A., et al. (2020). Green synthesis and characterization of zinc oxide nanoparticles with antibacterial and antifungal activity. *J. Mol. Struct*. 1211, doi: 0.1016/j.molstruc.2020.128107.

[25] ISO 6588-1:2021 (en) *Paper, board and pulps—Determination of pH of aqueous extracts*—Part 1: Cold extraction, Int. Stan. Pub., Geneva

[26] Ahmed, H., Mohamed, W., Saad, H., et al. (2017). Degradation behavior of nano-glue adhesive due to historical textiles conservation process. *Egyptian J. of Chemistry*. 60 (6): 1123-1133.

[27] El-Bisi, M., Ibrahim, H., Rabie, A., et al. (2016). Super hydrophobic cotton fabrics via green techniques. *Der Pharma Chem*. 8 (19): 57-69.

[28] ASTM D724-99 *Standard test method for surface wettability of paper (Angle-of-Contact Method)*, ASTM, USA.

[29] Periakaruppan, P., Gnanaprakasam, P., Emmanuel, R., et al. (2013). Green synthesis of silver nanoparticles from leaf extract of Mimusops lengi, Linn. for enhanced antibacterial activity against multi drug resistant clinical isolates. *Colloids & surfaces. B: Biointerfaces*. 108: 255-259.

[30] Alshammari, B., Alotaibi, M., Alothman, O., et al. (2019). A new study on characterization and properties of natural fibers obtained from olive tree (Olea europaea L.) residues. *J. of Polymers & the Environment*. 27: 2334-2340.

[31] Mansour, H., Shehata, M., Abdo, E., et al. (2023). Comparative analysis of silver-nanoparticles and whey-encapsulated particles from olive leaf water extracts: Characteristics and biological activity. *PlosOne*. 18 (12), doi: 10.1371/journal.pone.0296032.

[32] Nasir, G., Mohammed, A. & Abbas, Z. (2016). Biosynthesis and characterization of silver nanoparticles using olive leaves extract and sorbitol. *Int. J. of Scientific & Engineering Research*: 7 (1): 100-107.

[33] Berra, D., Laouini, S., Abderrhmane, B., et al. (2022). In vitro antioxidant activities of copper mixed oxide (CuO/Cu_2O) nanoparticles produced from the leaves of Phoenix dactylifera L. *Biomass Conversion & Biorefinery*. 14 (5) 6567-6580.

[34] Huzyan, H., Abdul Aziz, A. & Hussin, M. (2021). Ecofriendly wood adhesives from date palm fronds lignin for plywood. *BioResources*. 16 (2): 4106-4125.

[35] Mahdi, A., Abd, A. & Awad, K. (2022). The role of nano-selenium in alleviating the effects of salt stress in date palm trees (*Phoenix dactylifera* L.): A Fourier transform infrared (FTIR) spectroscopy study. *BioNanoScience*. 13 (7), doi: 10.1007/s12668-022-01046-1.

[36] Berra, D., Laouini, S., Boubaker, B., et al. (2018). Green synthesis of copper oxide nanoparticles by *Phoenix dactylifera* L leaves extract. *Digest J. of Nanomaterials and Biostructures*. 13 (4): 1341-1350.

[37] Matykiewicz, D., Barczewski, M., Mysiukiewicz, O., et al. (2021). Comparison of various chemical treatments efficiency in relation to the properties of flax, hemp fibers and cotton trichomes. *J. of Natural Fibers*. 18 (5): 735-751.

[38] Darwish, S., Hassan, R., Abou El Fottouh, A., et al. (2020). Evaluation the effectiveness of CMC and Klucel-E modified with TiO_2 and ZnO nanoparticles used for consolidation the damaged paper maps. *Int. J. of Science*: *Basic and Applied Research*. 52 (2): 217-232.

[39] Karthik, A., Bhuvaneshwaran, M., Kumar, M., et al. (2024). A review on surface modification of plant fibers for enhancing properties of biocomposites. *Chemistry Select*. 9 (21), doi: 10.1002/ slct.202400650.

[40] Abu Krorra, A., Noshy, W., Oun, A., et al. (2021). Evaluation of hydroxypropyl cellulose, zinc oxide nanoparticles and nanocellulose for tracing papers consolidation. *ARCS J.*: 2 (1): 21-30.

[41] Jalali, E., Erasmus, E., Schutte-Smith, M., et al. (2024). Fixation of nanoparticles on fabric: Applications in general health management. *Materialstoday Communications*. 41, doi: 10. 1016/j.mtcomm.2024.110577.

[42] Essien, E., Atasie, V., Okeafor, A., et al. (2019). Biogenic synthesis of magnesium oxide nanoparticles using Manihot esculenta (Crantz) leaf extract. *Int. Nano Letters*. 10 (1): 43-48.

[43] Rout, A., Kar, J., Jesthi, D., et al. (2016). Effect of surface treatment on the physical, chemical, and mechanical properties of palm tree leaf stalk fibers. *BioResources*. 11 (2): 4432-4445.

[44] Mazen, B., Ismail, B., Hassan, R., et al. (2025). Use of carboxymethyl cellulose, Klucel G, gum Arabic and zinc oxide nano-particles nanocomposite as strength agents for inked papyrus. *Pigment & Resin Technology*. 54 (2): pp. 224-239.